AIP | Review of Scientific Instruments

A portable quartz micro balance for physical vapor deposition techniques

S. Stuckenholz, C. Büchner, G. Thielsch, M. Heyde, and H.-J. Freund

Citation: Review of Scientific Instruments **84**, 085118 (2013); doi: 10.1063/1.4819030
View online: http://dx.doi.org/10.1063/1.4819030
View Table of Contents: http://scitation.aip.org/content/aip/journal/rsi/84/8?ver=pdfcov
Published by the AIP Publishing

Re-register for Table of Content Alerts

Create a profile.

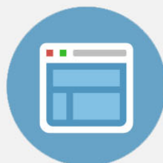

Sign up today!

This article is copyrighted as indicated in the article. Reuse of AIP content is subject to the terms at: http://scitationnew.aip.org/termsconditions. Downloaded to IP: 141.14.132.216 On: Mon, 27 Jan 2014 14:20:19

REVIEW OF SCIENTIFIC INSTRUMENTS **84**, 085118 (2013)

A portable quartz micro balance for physical vapor deposition techniques

S. Stuckenholz,[a] C. Büchner, G. Thielsch, M. Heyde,[b] and H.-J. Freund
Fritz-Haber-Institut der Max-Planck-Gesellschaft, Faradayweg 4-6, D-14195 Berlin, Germany

(Received 20 June 2013; accepted 8 August 2013; published online 27 August 2013)

A portable quartz crystal micro balance for physical vapor deposition techniques is presented. The device is used for the calibration of evaporators employed in the preparation of thin film systems that are studied in surface science. The design is based upon a portable sample setup, highly versatile and customizable. It can be transported within an ultrahigh vacuum system, stored in a sample garage and be used in front of different evaporators. Details of the setup are described. Finally, the performance of the device is demonstrated and compared to scanning tunneling microscopy measurements.
© *2013 AIP Publishing LLC*. [http://dx.doi.org/10.1063/1.4819030]

I. INTRODUCTION

Surface science studies require well-defined surfaces. Typical sample systems consist of thin films deposited on metal single crystal supports. These thin films can be deposited with various techniques, for example physical vapor deposition (PVD), chemical vapor deposition (CVD), and molecular beam epitaxy (MBE) based methods.[1,2]

In our department we study metal supported thin oxide films to understand fundamental principles of heterogeneous catalysis. The properties of these thin film systems highly depend on the used materials and on the oxide film thickness.[3] To study the structure-property-relationship a high control over the sample preparation process is required.

In order to prepare defined and reproducible films, the employed deposition techniques need to be calibrated. One method used to measure the film thickness in surface science and semiconductor technology is reflection high energy electron diffraction (RHEED).[4,5] Here, the film growth can be observed *in situ*. Other *in situ* methods that allow to monitor thin film growth in real space are low energy electron microscopy (LEEM) and photo-emission electron microscopy (PEEM).[6,7]

In former studies we used scanning tunneling microscopy (STM) or non-contact atomic force microscopy (nc-AFM) to analyze film coverages. With this approach, the coverage can be measured very accurately. However, these methods are quite time consuming.

A widely used method to monitor deposited amounts are quartz crystal sensor devices, also known as quartz crystal micro balances (QMB). Here, the changes of the resonance frequency of a quartz crystal are used to detect mass changes in the range of sub-nanograms.[8] Usually, QMBs are attached opposite to the evaporator in the ultrahigh vacuum (UHV) setup. Although there are ways to take off-centered positions of a QMB into account, it is favorable to measure the flux directly at the sample position. In the UHV setup presented here, various new material systems can be prepared and studied with several surface science techniques at different positions in one chamber system. This demands a high flexibility of all setup components and it is only possible with some portable elements, such as an incorporated portable sample setup. This is a common principle in UHV science and it has already inspired the design of other movable UHV equipment[9] and portable devices, e.g., portable evaporators.[10,11] Recently, we developed a portable QMB that can be placed in front of differently located evaporators, at the same position where the sample is placed during deposition. The presented portable QMB device highly advances the flexibility of UHV setups. It facilitates a quick analysis of the deposition rate (deposited evaporant amount per time unit) and of the ideal sample location for deposition.

II. EXPERIMENTAL SETUP

The experimental setup operates under UHV conditions. Sample preparation and analysis is combined in one system. This system consists of a preparation chamber that is directly connected to a main chamber which houses a dual mode nc-AFM/STM. The microscope setup is described in detail elsewhere.[12] The preparation chamber, see Fig. 1, is equipped with a rotatable manipulator (1). A clamping mechanism enables sample change under UHV conditions. A view port (7) is incorporated. The sample garage (2) can store up to four different samples. A heater, a sputter gun (6), and two triple evaporators (3, 4) are available for sample preparation. Different gaseous species can be dosed from a dispenser unit located between the preparation chamber and the main chamber. A valve can be closed between the gas dispenser (8) and the preparation chamber. A first analysis of sample preparations is done using a low energy electron diffraction (LEED) and Auger electron spectroscopy (AES) analysis system (5). The pumping unit is located below the chamber.

The portable QMB can be moved in the manipulator to any position desired. Hence, the best sample position for deposition can be identified easily. After usage the QMB is stored in the sample garage. In the conventional QMB setup, two QMB units would have to be mounted opposite the two evaporators that are used in this chamber, thus occupying two separate flanges. Further, the evaluation of this QMB data would require a correction for the different positions of the QMB and the sample, potentially inducing errors.

[a] Also at FU-Berlin, Fachbereich Biologie, Chemie, Pharmazie, Takustr. 3, D-14195 Berlin, Germany.
[b] Electronic mail: heyde@fhi-berlin.mpg.de

This article is copyrighted as indicated in the article. Reuse of AIP content is subject to the terms at: http://scitationnew.aip.org/termsconditions. Downloaded to IP: 141.14.132.216 On: Mon, 27 Jan 2014 14:20:19

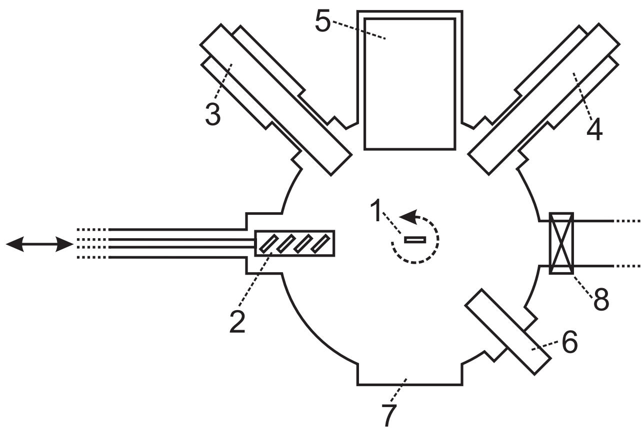

FIG. 1. Schematic drawing of the UHV preparation chamber: (1) rotatable manipulator, (2) manipulator with sample garage, (3) and (4) triple evaporators, (5) LEED/AES optics, (6) sample heater/sputter gun, (7) view port, and (8) a valve connecting the preparation chamber with the main chamber, which houses the STM and AFM setup.

The assembly of the portable sample holder, as well as of the portable QMB setup are shown in Fig. 2. In the sample holder (Fig. 2(a)), a metal single crystal is mounted with two molybdenum sheets on a sapphire carrier. At the top, the K-type thermocouple wires are attached to a sapphire carrier and connected to the crystal. Two metal protrusions on the front and two on the back side of the metal support are used to hold the sample in the manipulator clasp. This typical sample setup demonstrates the limitations for the new QMB setup. The manipulator provides two separate contacting channels; one via the clasp, the second via the thermocouple wires. These are used for the electrical connections. No extra wiring is attached to the manipulator, making this design applicable to all clasp-manipulators with thermocouple wiring and one additional electrical connection. The QMB's outer dimensions should not exceed those of the portable sample holder outer dimensions.

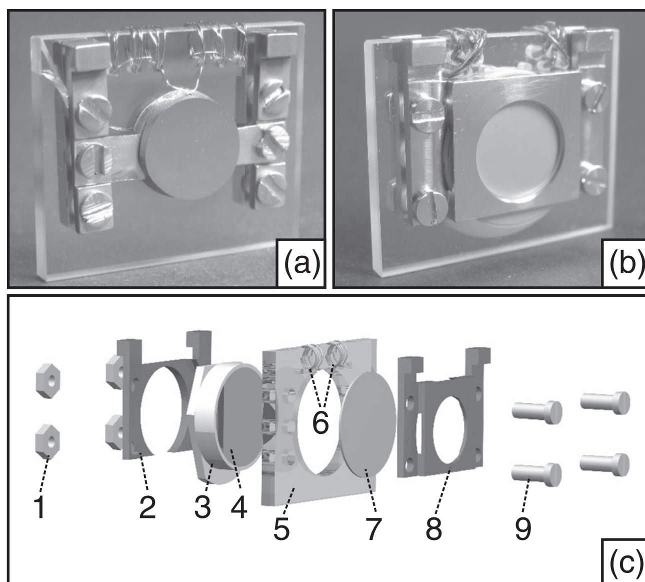

FIG. 2. Photograph of (a) a NiAl(110) single crystal in a standard sample holder and of (b) the portable QMB. Each mounted on a supporting sapphire with edge lengths of $(20 \times 25 \times 2)$ mm^3. (c) Schematic of the disassembled QMB, showing the single parts used: (1) nuts, (2) metal back support, (3) ceramic housing containing (4) back-contact-springs, (5) sapphire support, (6) thermocouple wires, (7) gold coated quartz crystal, (8) supporting front contact, and (9) screws.

In Fig. 2(b), a photograph of the assembled portable QMB is shown. Figure 2(c) depicts the single parts of the portable micro balance device. The commercial gold coated sensor crystal (7) has a resonance frequency of 6 MHz (MDC Vacuum Products LLC) and is electrically connected via the front metal support (8) to the manipulator clasp. The back of the quartz crystal is connected via the back-contact-springs (4) in a ceramic housing (3) to the K-type thermocouple wires ($\oslash = 0.2$ mm) (6). An additional metal frame in the back (2) is mechanically supporting the back-contact. Nuts (1) and screws (9) are used to fasten the device.

A BNC connection carries the power and the signal path to and from the oscillating crystal. Signal ground is applied at the back of the crystal sensor using the thermocouple contact, whereas the signal connection to the crystal front side is provided via the manipulator clasp. The crystal sensor device is electrically connected to a thickness/rate monitor (STM-100/MF, Sycon Instruments) using the BNC connection. The use of shielded cables is recommended. In our setup, only the ex-vacuum cables are shielded.

For a stable and reproducible measurement with the QMB device, a constant temperature is very important. Hence, it is also recommended to water-cool the sensor device. Although cooling is possible in many manipulators, we operated the portable QMB at room temperature without cooling.

Different applications of the QMB measurements are possible, three will be described here. The first method, especially useful in the case of co-deposition, is the so-called spot profiling. Here, the monitored deposition rate is correlated with the position of the QMB.

Second, the stability of the evaporation and of the thickness measurement are checked. These measurements are performed by closing and opening the evaporator shutter successively and determining the respective deposition rates. These first two measurements were performed with Mg (in a crucible) evaporated from a Knudsen-cell.

Finally, we compared the monitored deposition rates of Si (evaporated from a Si-rod) with an STM coverage analysis of a silica film, before and after maintenance of an evaporator unit, qualitatively and quantitatively.

III. RESULTS

The QMB is picked up with the manipulator clasp and positioned so that a steady contact to the thermocouple wires is ensured. To minimize thermal drift no sample-heating is performed in the clasp several hours prior to deposition experiments. Signal stability is improved by starting the thickness/rate monitor an hour before measuring.

The above mentioned routine was used in all of the measurements presented here. The used evaporators (EFM Series, Omicron Nanotechnology) detect a flux of evaporated ions internally. This signal can be used as a qualitative measure of

This article is copyrighted as indicated in the article. Reuse of AIP content is subject to the terms at: http://scitationnew.aip.org/termsconditions. Downloaded to IP: 141.14.132.216 On: Mon, 27 Jan 2014 14:20:19

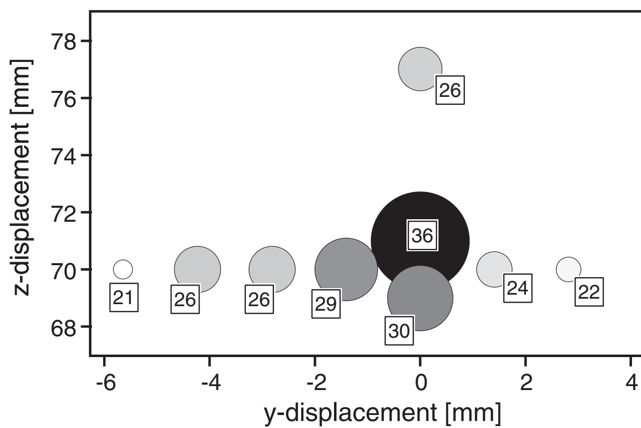

FIG. 3. Monitored deposition rate versus QMB position. Different y- and z-displacements on a plane orthogonal to the evaporator beam were tested. Each symbols' center indicates the measurement position, its diameter scales linearly with the deposition rate in Å/min, indicated in the labels. To guide the eye, a gray scale visualizes the deposition rate value.

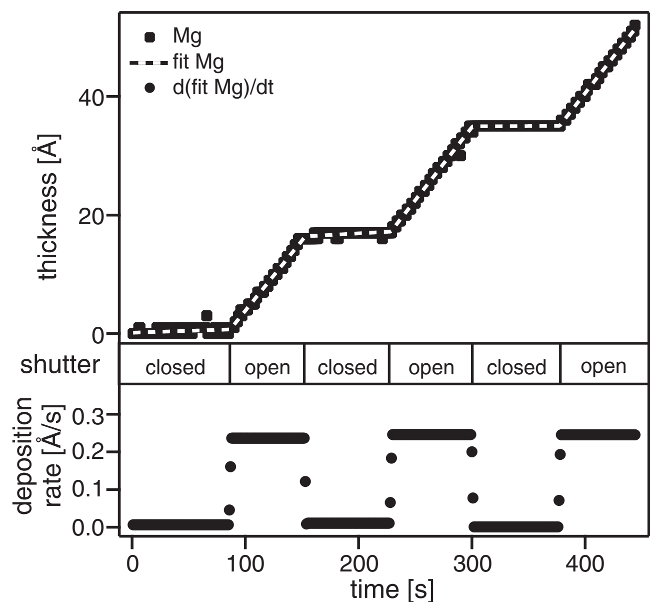

FIG. 4. Monitored thickness and the sequenced linear thickness fit with respect to the evaporation time and the deposition rate with respect to the deposition time. The evaporator shutter was closed or open, as indicated, respectively.

the evaporated material amount. Constant evaporation is usually reached after several minutes of evaporation indicated by a constant ion flux.

The evaporators used for thin film deposition produce a spot diameter of approximately 10 mm. Typically, the samples are circular metal disks with a diameter ranging between 7 and 10 mm. Hence, knowing the exact evaporator spot profile is necessary for a good positioning and thus a homogeneous deposition on the sample. Especially in the case of co-deposition, where two or more elements are deposited at the same time, knowledge about the spot profile helps to find the ideal sample position.

The results of a spot profile experiment performed with Mg evaporated from a Knudsen-cell are displayed in Fig. 3. The deposition rates were monitored at different spots in front of the evaporator, while keeping the evaporator parameters constant. The position of the sensor device was adjusted in two dimensions, namely, a horizontal y- and a vertical z-direction. The symbol center indicates each measurement position with coordinates (y, z). The diameter of each symbol scales linearly with the deposition rate which is given in Å/min in the label. Additionally a gray scale visualizes the deposition rate. The spot profile shows a maximum deposition rate for the QMB position at (0 mm, 71 mm). The measured rate decreases continuously in all four tested directions. Since the QMB location is exactly the same as the sample position, the results can be directly used for optimizing the preparation. The data presented here indicate a small spot profile and a sample position at (0 mm, 71 mm) should be used for further depositions when using the Mg evaporator.

As an example for the calibration of an absolute deposition rate, we evaporated Mg from a Knudsen cell onto the portable QMB, see Fig. 4. Again, the ion flux value was kept constant during the experiment. The monitored Mg thickness (Mg) is represented by black squares. The shutter was opened and closed successively, for a defined time frame, as indicated in the figure. A sequenced linear fit of the deposited Mg amount for the duration of each time frame (fit Mg) is visualized by a dashed line. The lower part of the figure shows the Mg deposition rate in Å/s, determined as $d(fit\ \mathrm{Mg})/dt$. A comparison of the deposition rates during closed shutter periods, which are close to zero, show a low drift of the QMB measurement. The similar rates during open shutter intervals indicate homogeneity of the evaporator Mg flux. This experiment allows to compare the qualitative ion flux monitor value of the evaporator with an absolute deposition rate value.

Quantitative deposition analyses like the examples presented have to be repeated on a regular basis. After several cycles of sample preparation, depending on the evaporated amount, a depletion of the evaporant material might lead to a change of the evaporation rate. The evaporation rate and the ion flux signal also change with every modification of the evaporator geometry. These modifications are often the result of evaporator maintenance, such as refilling and repositioning of a crucible/evaporant-rod, or cleaning of the evaporator.

The Si-evaporator calibration was done using two independent methods, each applied before and after a maintenance procedure.

The first method used the STM-based image analysis, see Figures 5(a) and 5(b). The precision of the STM-based coverage analysis mainly depends on the tip apex curvature,[13] statistical and systematical errors of the image analysis. Images of several different sample regions with a high contrast were evaluated for the coverage analysis, leading to an estimated error of 1% of the evaluated coverage.

For both experiments, we employed a recipe for a silica sub-monolayer coverage on Ru(0001) before and after maintenance. An ion flux of 15 nA was used and we deposited Si for 5 min, followed by an annealing step in oxygen atmosphere to produce silica. The detailed recipe for silica film preparations has been reported in Ref. 14.

As second calibration method, the Si-deposition rate was measured with the QMB device, before and after maintenance

This article is copyrighted as indicated in the article. Reuse of AIP content is subject to the terms at: http://scitationnew.aip.org/termsconditions. Downloaded to IP: 141.14.132.216 On: Mon, 27 Jan 2014 14:20:19

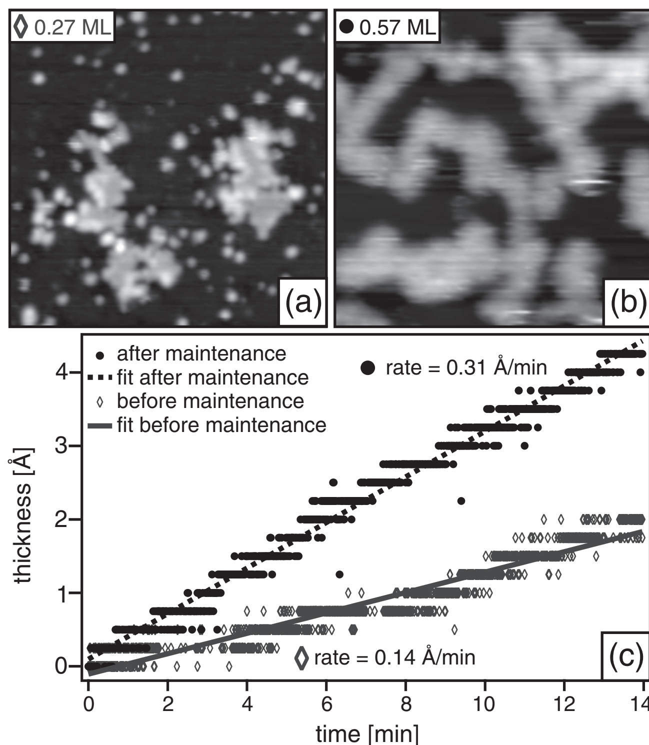

FIG. 5. (a) and (b) STM images of silica sub-monolayer coverages on Ru(0001) prepared with the same recipe. The results (a) before maintenance (b) after maintenance of the used Si-evaporator unit are shown here. The coverage, evaluated with STM images of several surface positions for each preparation, is given in monolayers (ML) in the upper left corner of the presented images. (c) QMB measurements. Monitored thickness of Si on the sensor crystal surface with respect to the evaporation time. The linear fits of the data and the evaporation rates are indicated in the graph. Symbols are used to distinguish measurements before the maintenance (diamond outline, gray) and after the maintenance (filled circle, black).

(see Fig. 5(c)). Here, an ion flux of 25 nA was used. The data acquired with the QMB sensor were linearly fitted to obtain the Si evaporation rate given in Å/min.

The STM method amounts to a factor of $\frac{0.57\,ML}{0.27\,ML} = 2.1$ for the silica coverage. The QMB method evaluation results in a factor of $\frac{0.31\,\text{Å/min}}{0.14\,\text{Å/min}} = 2.2$ for the deposition rates. The determined factors deviate less than 5%, indicating a satisfactory qualitative agreement between the STM-based and the QMB-based technique.

To compare the results of QMB and STM quantitatively, an expected silica coverage can be calculated from the monitored Si rate (QMB). The calculated expected coverage is then compared to the coverage analysis value (STM). In this experiment, we prepared a fraction of a silica monolayer (*ML*). The *ML* has a stoichiometry of $SiO_{2.5}$.[15] However, a *ML* consists of half the amount of Si atoms compared to a silica bilayer (*BL*). The density of pure Si is known to be $\rho_{\mathrm{Si}} = 2.33\,\frac{\mathrm{g}}{\mathrm{cm}^3}$, and the two-dimensional mass density (2D-density) of a *BL* was recently evaluated to be $\rho_{BL} = 1.65\,\frac{\mathrm{mg}}{\mathrm{m}^2}$.[16,17]

Further, it is assumed that in the considered range the ion flux monitor data scales linearly with the deposited amount of Si and that no Si evaporates during the oxidation step to form silica.

With the previously mentioned values and assumptions, the calculated expected silica coverage, before maintenance, results in 0.25 *ML*. Further calculation details can be found in Ref. 18. The calculated value deviates by 0.02 *ML* from the STM-based result of 0.27 *ML*.

The same calculations made for the expected silica coverage after maintenance, result in an expected coverage of 0.56 *ML*.[19]

After maintenance, the STM-analyzed coverage was 0.57 *ML*, which is 0.01 *ML* higher than the calculated QMB-based result.

This calculation allows to quantitatively compare the data of the STM-based coverage analysis and the QMB deposition measurements. The numbers show a good compliance, deviating only 0.02 *ML* and 0.01 *ML* between the calculated and the observed coverage values. Hence, the more rapid calibration of an evaporator with the portable QMB device yields results that are comparable to an STM-image analysis procedure.

IV. CONCLUSIONS

A customizable way of implementing a quartz sensor device is presented. The portable QMB can be introduced into any setup providing two separate electrical contacts at the manipulator clamp. In this manner, the QMB can be positioned like any sample, hereby enhancing the flexibility for performing experiments in the UHV chamber. QMB and STM measurements are presented, demonstrating the capabilities of the said setup.

The sensor sensitivity allows the calibration of deposition rates below 0.2 Å/min. Hence, an application for ultrathin films (few atomic layers) as well as for thicker films is possible.

The deposition rate analysis with a QMB is faster compared to analysis using STM data with good quantitative agreement.

In addition to general evaporator calibration, a portable setup allows for spot-profiling experiments.

ACKNOWLEDGMENTS

S.S. would like to acknowledge the support from the Deutsche Forschungsgemeinschaft (DFG) through the Cluster of Excellence Unifying Concepts in Catalysis (UNICAT).

1. H. Lüth, *Solid Surfaces, Interfaces and Thin Films*, Graduate Texts in Physics (Springer, Berlin, Heidelberg, 2010).
2. J. A. Venables, *Introduction to Surface and Thin Film Processes* (Cambridge University Press, Cambridge, 2000).
3. H.-J. Freund, Chem.-Eur. J. **16**, 9384 (2010).
4. S. A. Chambers, Surf. Sci. Rep. **39**, 105 (2000).
5. P. I. Cohen, J. Vac. Sci. Technol. A **4**, 1251 (1986).
6. E. Bauer, Rep. Prog. Phys. **57**, 895 (1994).
7. A. Locatelli and E. Bauer, J. Phys.: Condens. Matter **20**, 093002 (2008).
8. G. Sauerbrey, Z. Phys. **155**, 206 (1959).
9. J. T. Yates, Jr., *Experimental Innovations in Surface Science* (AIP/Springer, New-York, 1998).
10. H.-P. Rust, T. König, G. H. Simon, M. Nowicki, V. Simic-Milosevic, G. Thielsch, M. Heyde, and H.-J. Freund, Rev. Sci. Instrum. **80**, 113705 (2009).
11. K. Lämmle, A. Schwarz, and R. Wiesendanger, Rev. Sci. Instrum. **81**, 053902 (2010).
12. M. Heyde, G. H. Simon, H.-P. Rust, and H.-J. Freund, Appl. Phys. Lett. **89**, 263107 (2006).
13. J. S. Villarrubia, J. Res. Natl. Inst. Stand. Technol. **102**, 425 (1997).

This article is copyrighted as indicated in the article. Reuse of AIP content is subject to the terms at: http://scitationnew.aip.org/termsconditions. Downloaded to IP: 141.14.132.216 On: Mon, 27 Jan 2014 14:20:19

[14]L. Lichtenstein, C. Büchner, B. Yang, S. Shaikhutdinov, M. Heyde, M. Sierka, R. Włodarczyk, J. Sauer, and H.-J. Freund, Angew. Chem., Int. Ed. Engl. **51**, 404 (2012).

[15]L. Lichtenstein, M. Heyde, S. Ulrich, N. Nilius, and H.-J. Freund, J. Phys.: Condens. Matter **24**, 354010 (2012).

[16]*CRC Handbook of Chemistry and Physics: A Ready-Reference Book of Chemical and Physical Data*, 91st ed., edited by W. M. Haynes and D. R. Lide (CRC Press, Boca Raton, FL, 2010).

[17]M. Heyde, G. H. Simon, and L. Lichtenstein, Phys. Status Solidi B **250**, 895 (2013).

[18]To calculate the 2D-density of pure Si in one *ML* ($\rho_{\mathrm{Si}ML}$), we use a simple stoichiometry approach (atomic weights of Si = 28 amu and O = 16 amu and 60 amu for an equivalent of SiO_2). The fraction of Si in 0.5 *BL* can be calculated: $\rho_{\mathrm{Si}ML} = 1.65\,\frac{\mathrm{mg}}{\mathrm{m}^2} \times \frac{1}{2} \times \frac{28\,\mathrm{amu}}{60\,\mathrm{amu}} = 0.385\,\frac{\mathrm{mg}}{\mathrm{m}^2}$. The factor θ_{ML} gives us the deposited Si film thickness needed to produce one silica monolayer after oxidation, $\theta_{ML} = \frac{\rho_{\mathrm{Si}ML}}{\rho_{\mathrm{Si}}} = \frac{0.385\,\mathrm{mgm}^{-2}}{2.33\,\mathrm{gm}^{-3}} = 1.65\,\mathrm{Å}$. Before maintenance, the monitored deposition rate of Si, at an ion flux of 25 nA, was 0.14 Å/min. For an ion flux of 15 nA this equates to a deposited Si-film thickness of $\theta_{bm} = 0.14\,\frac{\mathrm{Å}}{\mathrm{min}} \times \frac{15\,\mathrm{nA}\times 5\,\mathrm{min}}{25\,\mathrm{nA}} = 0.42\,\mathrm{Å}$ after 5 min of Si-deposition. The calculated *ML* coverage, evaluated from the QMB measured deposition rate, is given by the fraction $\frac{\theta_{bm}}{\theta_{ML}} = \frac{0.42\,\mathrm{Å}}{1.65\,\mathrm{Å}} = 0.25$.

[19]$\frac{\theta_{am}}{\theta_{ML}} = \frac{0.93\,\mathrm{Å}}{1.65\,\mathrm{Å}} = 0.56$.

This article is copyrighted as indicated in the article. Reuse of AIP content is subject to the terms at: http://scitationnew.aip.org/termsconditions. Downloaded to IP: 141.14.132.216 On: Mon, 27 Jan 2014 14:20:19